Effects of numerical diffusion and mass conservation errors on turbulent transport of high Schmidt number scalars

Siddhartha Verma*, and G. Blanquart**
Corresponding author: sverma@caltech.edu

* Graduate Aerospace Laboratories, California Institute of Technology.
** Department of Mechanical Engineering, California Institute of Technology.

Abstract: We investigate the detrimental effects of various transport schemes on turbulent mixing of low diffusivity passive scalars, and recommend new grid resolution criteria to account for these. Several Eulerian and Semi-Lagrangian schemes are compared for their ability to predict accurately the expected turbulent behavior of the scalars. Scalar energy and dissipation spectra, as well as small-scale scalar statistics provide a comprehensive picture of the strengths and shortcomings of the schemes tested. We show that for standard Eulerian transport schemes, a resolution of up to $\kappa_{max}\eta_B = 3$ might be necessary for sufficient accuracy. However one of the Semi-Lagrangian schemes tested (MECH) is capable of producing comparable results at $\kappa_{max}\eta_B = 1.5$. This allows for a significant reduction in computational cost without sacrificing accuracy.

Keywords: Turbulent Mixing, High Schmidt, Numerical Diffusion, DNS, scalar transport, Semi-Lagrangian.

1 Introduction

The grid resolution required for fully resolving high Schmidt number turbulent simulations is determined by the Batchelor scale ($\eta_B = \eta/\sqrt{Sc}$), which in turn depends on the Kolmogorov length scale (η), and the Schmidt number (Sc). The Schmidt number is defined as the ratio of the kinematic viscosity of the fluid (ν) and the molecular diffusivity of the passive scalar ($Sc = \nu/D$). A passive scalar is any physical quantity that is convected under the influence of the velocity field, but has no effect on the velocity itself. Some examples include small temperature fluctuations in air and water, and pollutant (e.g. soot) or contaminant transport in the atmosphere and the ocean. The extremely small value of the Batchelor scale for high Schmidt number simulations necessitates the use of very fine grids to capture the physically important small scale structures. The need for high accuracy at these small scales makes the simulations extremely sensitive to numerical diffusion.

Commonly accepted guidelines suggest that keeping $\kappa_{max}\eta_B \geq 1.5$, where κ_{max} is the largest wavenumber determined by the grid size (N), ensures a fully resolved scalar field [1]. However, resolving all the physically important scales does not necessarily guarantee that discretization errors from the numerical scheme used will not have an appreciable adverse effect on the results. For instance, using the scalar dissipation spectra plotted in Fig. 1 , we can observe the considerable impact that numerical diffusion has on the smaller scales. The aforementioned grid resolution criterion ($\kappa_{max}\eta_B = 1.5$) is satisfied for $N = 256$. However, we see a large discrepancy (for $\kappa\eta \geq 4$) when we compare the finite-volume results to those generated by a spectral code. Refining the grid to $N = 512$ leads to better agreement, but at a cost increase of 16 times. These results clearly indicate that the currently established resolution criteria for ensuring the physically accurate simulation of high Schmidt scalar transport may need to be revised.

Turbulent simulation of low diffusivity passive scalars (e.g. soot) requires that numerical diffusivity of the transport scheme used be kept to a minimum to avoid contamination of transport characteristics. In
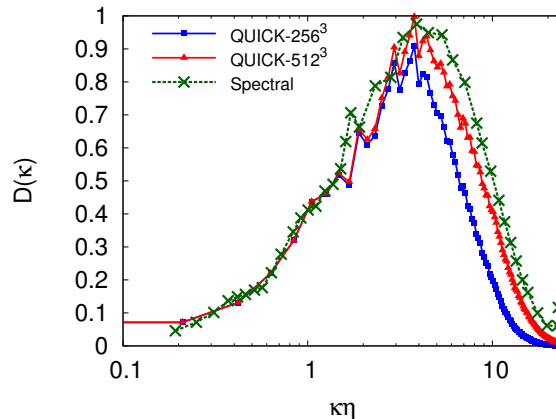
Figure 1: Normalized dissipation spectra showing the effect of numerical diffusion ($\text{Re}_\lambda \approx 8$, Sc= 256). "Spectral" data taken from [1].

addition, boundedness of scalar quantities, for example species mass fraction between 0 and 1, is essential to keep the simulations physically relevant. Unfortunately, these two properties often show mutually conflicting behavior. Ensuring the boundedness of Eulerian transport schemes (e.g. WENO [2], BQUICK [3]) introduces significant numerical diffusion. Nonetheless, finite-volume Eulerian schemes have traditionally been preferred over Semi-Lagrangian (SL) approaches with lower diffusion, since they ensure conservation [4]. Numerical diffusion can be mitigated by using higher-order accurate methods, however the corresponding increase in computational cost is often significant.

We present an analysis of the various effects that both numerical diffusion, and non-conservative transport have on high Schmidt number turbulent mixing. The numerical schemes used are discussed in Section 2, followed by an analysis of their performance in laminar (Section 3.1), and turbulent (Section 3.2) flows. The focus is on the ability of the schemes to predict correctly the expected scalar spectra (energy, and dissipation) (Section 3.2.1, Section 3.2.2) and small-scale turbulent statistics (Section 3.2.3). The results are used to propose new grid-resolution guidelines that account for sensitivity to numerical diffusivity of the scheme used.

2   Numerical Methods

Traditionally, spectral schemes have been preferred over finite-volume (FV) and finite-difference (FD) schemes for studying characteristics of turbulent flow [5, 6, 7]. The reason for this is the exponential drop in discretization error associated with spectral schemes [8]. However there are certain limitations to using these schemes. The occurence of Gibb's phenomenon near sharp jumps in the scalar field, which are a common occurence in high Schmidt number transport, makes it impossible to maintain scalar boundedness. Additionally, the use of Fourier transforms makes it necessary to work with periodic boundary conditions. This last point renders spectral schemes unsuitable for studying many engineering applications, such as simulations of flow inside a combustion chamber, since these require working with complex geometries and boundary conditions. FD and FV schemes are an attractive alternative to spectral schemes in that they do not suffer from these two limitations. These schemes, however, present other issues, such as a comparatively lower order of accuracy, and the occurence Runge's phenomenon when using high order polynomial interpolation [9]. Runge's phenomenon can be largely minimized by using Hermite interpolation [10] since the derivatives are now constrained at node points. The use of Hermite interpolation in the current work is also shown to lead to much better accuracy compared to using Lagrange polynomials [10].

2.1 Desirable Properties of Transport Schemes

Some of the most important properties of transport schemes are their ability to maintain 1) high accuracy, 2) conservation, 3) minimal numerical diffusion, and 4) monotonicity (or boundedness). It is often the case that certain properties, like boundedness and accuracy, are sacrificed in favor of other properties. This can cause severe problems in situations where non-monotonic behavior leads to unphysical situations. For instance, allowing temperature values, or species mass fraction in reacting flows to become negative can have significant detrimental effects on the solution of the partial differential equations. In other situations, such as long-term weather and climate simulations, mass conservation can be the paramount issue [11]. Several authors have noted that monotonicity is valuable in theses simulations as well [12], since allowing quantities like water vapor content to become negative can lead to unphysical results.

2.2 Eulerian schemes

As mentioned earlier, Eulerian FV schemes are inherently mass conservative, which makes them the preferred choice for a majority of numerical work conducted. These schemes, however, suffer from other shortcomings. We conduct tests for two commonly used Eulerian transport schemes, namely QUICK [13] and BQUICK [3], to analyze the effect of the associated numerical errors on turbulent scalar transport. Of these, only BQUICK is monotonicity preserving. To maintain monotonicity, BQUICK employs a flux limiting procedure in the QUICK framework, whenever the calculated value exceeds the specified upper and lower bounds.

2.3 Semi-Lagrangian (SL) schemes

Semi-Lagrangian schemes offer an attractive alternative to Eulerian schemes, on account of reduced numerical dispersion and dissipation errors. The basic idea behind the workings of SL schemes is discussed by Purser and Leslie in their 1991 paper [14]. Each Eulerian grid point is first traced back to its corresponding Lagrangian point at the previous time step. Then, an appropriate interpolation method is used to determine the scalar content of this Lagrangian particle. The particle is advected back to the Eulerian grid point according to the incompressible material transport equation (Eq. 1, with $\mathcal{D} = 0$). Finally, the effects of the diffusion term are accounted-for using a fractional-step method (Godunov splitting). Boundedness is applied before the fractional step accounting for the source and sink terms, since the advection step alone can produce non-monotonic behavior.

$$\frac{Dz}{Dt} = \mathcal{D}\nabla^2 z \tag{1}$$

$$\Rightarrow \frac{\partial z}{\partial t} + \mathbf{u} \cdot \nabla z = \mathcal{D}\nabla^2 z \tag{2}$$

In the current work, a second order Runge-Kutta (RK2) integrator was used for trace-back in the SL schemes. A fourth order Runge-Kutta (RK4) integrator was seen to lead to only a marginal improvement in accuracy. The RK2 integrator was thus preferred due to its comparatively lower computational cost. Two different interpolation methods were used for reconsturcting the scalar content of the traced-back Lagrangian particle. The first method used a 4-point stencil to construct a cubic Lagrange polynomial (SL3). The second method used a compact 2-point stencil for performing cubic Hermite interpolation (MonotonE-Cubic Hermite interpolation: MECH). MECH requires derivative values of the scalar field at the grid nodes. A second order central difference was thus used to re-calculate the required derivatives at every timestep. Monotonicity is maintained in SL3 by switching to linear interpolation whenever the specified bounds are exceeded. MECH, on the other hand, uses derivative limiting as explained by Fritsch and Carlson [15], to ensure monotonicity. There can be instances when the interpolated value exceeds the bounds even after applying the derivative limiters. In such cases, the derivatives at both nodes are set to zero, which ensures boundedness unconditionally.

The interpolation procedure in both SL3 and MECH is non-conservative. The bounding procedure can introduce additional non-conservative effects. A loss in conservation can be modeled physically using source terms, however unbounded species concentrations cannot. We therefore suggest that it is preferable to allow a minimal error in mass conservation, rather than to allow unphysical errors. There have been several

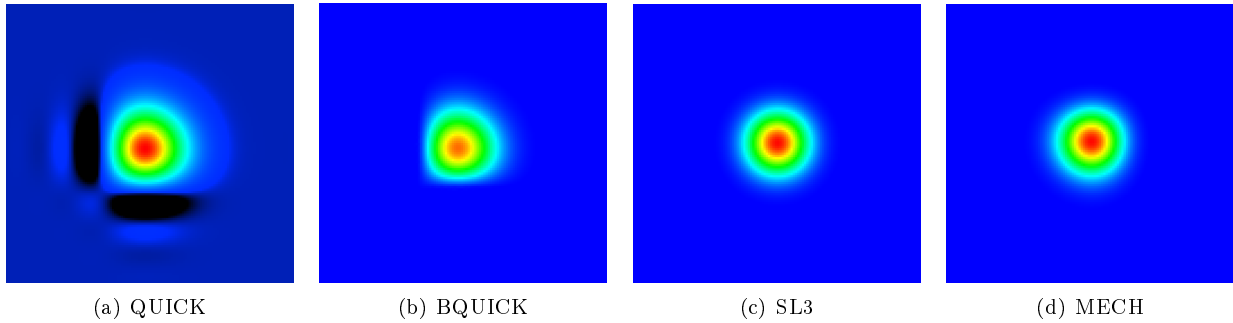(a) QUICK (b) BQUICK (c) SL3 (d) MECH

Figure 2: Pure convection of a passive scalar (Gaussian bell-shaped distribution). Results shown after 10 rotations. Color-map for the QUICK scheme has been rescaled to show negative oscillations in black.

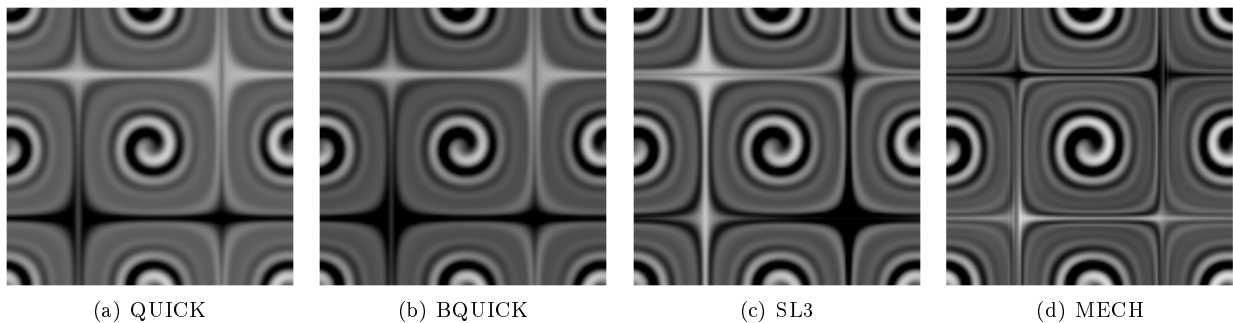(a) QUICK (b) BQUICK (c) SL3 (d) MECH

Figure 3: Taylor-Green vortex simulation with sinusoidal initial distribution of the scalar.

efforts in the past to make SL schemes conservative. However, these introduce certain anomalous effects, such as failing to maintain the transport of a constant field (e.g., the scheme proposed by Lentine *et.al.* [16]), or are so prohibitively expensive (remapping techniques [17]) that they are routinely used only for 2D simulations. Other attempts, such as those by Xiao *et.al.* [18] are both bounded and conservative, but end up inadvertently introducing significant numerical diffusion, or sacrificing the order of accuracy of the scheme.

3   Results

3.1   Laminar Flows

To study qualitatively the effect of the schemes on the transport characteristics of a passive scalar, we first select two simple laminar cases that are representative of the small scale motion of turbulent eddies. These simulations were run with zero molecular diffusivity, and all the noticeable diffusive effects are purely numerical. The first case (Fig. 2) corresponds to pure convection of a Gaussian bell-shaped scalar distribution along the 45-degree diagonal. The QUICK scheme is clearly unbounded, and the scalar attains negative values in a relatively large region. Excessive diffusion is noticeable for BQUICK, and is caused by switches to linear interpolation for maintaining boundedness. Dispersion errors are clearly discernible in the results of the Eulerian schemes, and are caused by upwinding during reconstruction of the cell face flux values. Upwinding is required for keeping the Eulerian simulations stable (i.e., non-oscillatory). On the other hand, the SL3 and MECH schemes, which use centered stencils, are seen to exhibit minimal numerical dissipation and dispersion errors.

The second case (Fig. 3) consists of a Taylor-Green vortex, and is a simplistic representation of the stretching and straining motion of a scalar field by turbulent eddies. The initial profile corresponds to a sine wave in the x-direction. The QUICK scheme was seen to breach bounds at times, whereas BQUICK still proved to be too diffusive. The SL3 scheme performs better in lowering numerical diffusion, though
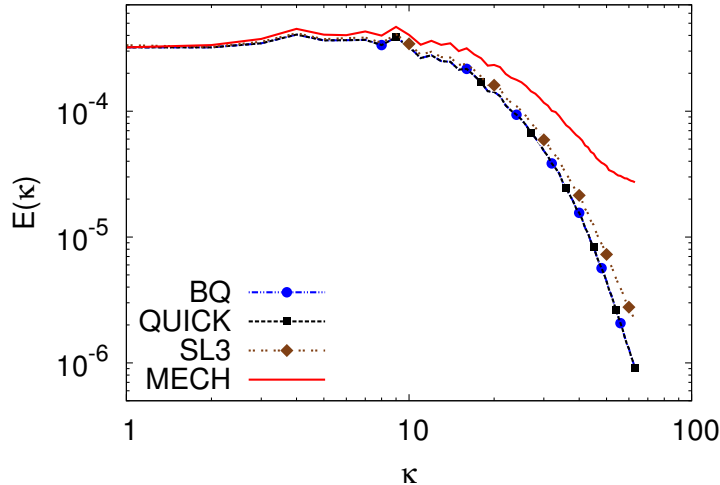
Figure 4: Energy spectra of decaying scalar field for $Re_\lambda = 30, Sc = \infty$

only marginally. We observe that the MECH scheme is superior to all other schemes in preserving the small scales. Although making a scheme monotone should make it inherently more diffusive, we note that the sub-cell shape-preserving nature of the Hermite interpolation makes MECH perform even better than the non-monotone QUICK scheme.

3.2   Turbulent Simulations

To assess the effect of the discretization errors on turbulent scalar transport, we conduct simulations in Homogeneous Isotropic Turbulence (H.I.T.) configurations. The simulations use a 3D periodic 'box' of length 2π, with an equal number of grid points in all three directions. The CFL (Courant-Friedrichs-Lewy) number is maintained smaller than 1 to ensure stability of the Eulerian schemes. The turbulent velocity field is forced spectrally by injecting energy in a low wavenumber shell [19]. The scalar field is maintained statistically stationary by imposing a uniform mean scalar gradient [7]. The simulations use successively finer grid resolutions to ascertain the optimal resolution for scheme independence of the results. Donzis *et.al.* [6] recently conducted a similar study on the effect of grid resolution on turbulent scalar statistics using a pseudo-spectral solver. The work presented in this paper focuses on the effect of the numerical scheme, as opposed to that of the grid resolution.

3.2.1   Turbulent Spectra (Sc=∞)

Energy and dissipation spectra of a scalar field can be used to gain insight into the effectiveness of the numerical scheme in maintaining the expected turbulence behavior. To observe the effect that numerical diffusion has on scalar spectra, we run simulations with zero molecular diffusivity. The initial scalar field in obtained by performing a simulation with both velocity and scalar forced, until statistical stationarity is achieved. As a second step, the mean gradient forcing is removed, molecular diffusivity set to zero ($Sc = \infty$), and the scalar field is allowed to decay. The resulting spectra are shown in Fig. 4. It is clear that the loss in scalar variance (z_v - integral area under the spectrum curve) is much higher for all the schemes when compared to the loss in MECH.

Fig. 5 shows a closer comparison between the spectra obtained using QUICK and MECH for several successive snapshots. The spectrum for MECH becomes flatter at later times, which is expected as the energy cascaded down to smaller scales is no longer dissipated by molecular diffusion. This leads to a pile up of energy at the small scales (which is evidence of low numerical diffusivity), and a more even distribution of energy among the wavenumbers. On the other hand, QUICK experiences significant numerical diffusion at larger wavenumbers, the effects of which affect the spectrum not only at the small scales, but also at
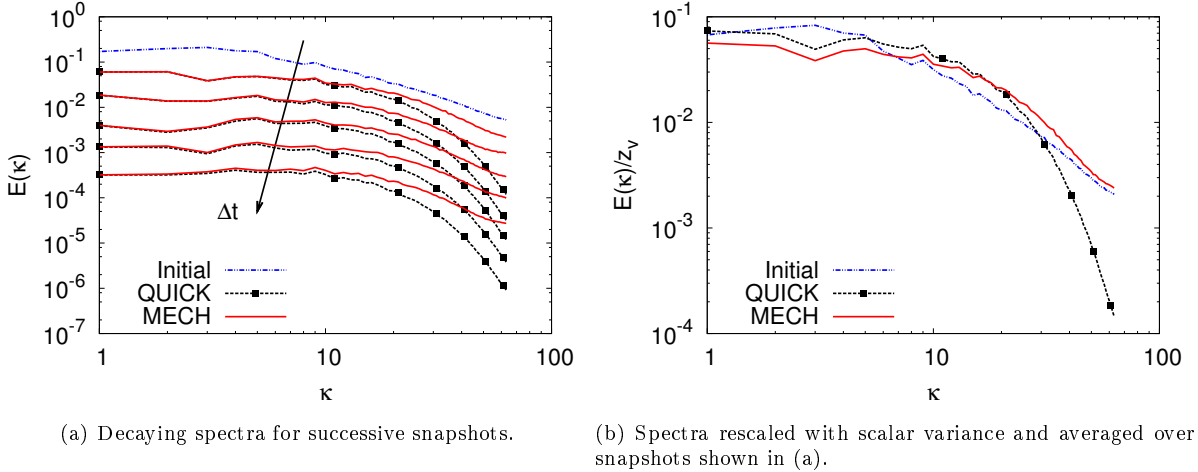
(a) Decaying spectra for successive snapshots.

(b) Spectra rescaled with scalar variance and averaged over snapshots shown in (a).

Figure 5: Decaying scalar energy spectra for $Re_\lambda = 30$, $Sc = \infty$

intermediate length scales (in the vicinity of $\kappa = 10$). This observation is crucial since it underlines the detrimental impact that numerical diffusion can have on the scalar transport characteristics.

3.2.2 Finite Schmidt Number simulations

Having established the detrimental role of numerical diffusion for zero diffusivity scalars, we now move on to statistically stationary H.I.T. simulations with finite Schmidt numbers. The intent is to investigate the effects of numerical diffusion on the scalar spectrum for finite Schmidt numbers, and ensure that these effects are not just limited to the $Sc = \infty$ case. We compare spectra obtained using different scalar schemes to that proposed by Kraichnan [20] for high Schmidt number scalars.

$$E(\kappa) = q\langle\chi\rangle(\nu/\langle\epsilon\rangle)^{1/2}\kappa^{-1}(1 + \kappa\eta_B\sqrt{6q})\exp(-\kappa\eta_B\sqrt{6q}) \qquad (3)$$

The Kraichnan form (K-Form) introduces a correction to the spectrum form initially proposed by Batchelor [21], by accounting for intermittent fluctuations in the strain-rate. This has been shown to give better agreement with available experimental and simulation data in the viscous-diffusive subrange. The value for the parameter $q = 2\sqrt{5}$ was derived using theoretical considerations by Qian [22]. Fig. 6 shows comparisons of the spectra at $Re_\lambda = 30$ (where λ is the Taylor microscale) and $Sc = 4$ for the various schemes. The comparisons are made at three grid resolutions corresponding to $\kappa_{max}\eta_B = 1.5$ (N= 128^3), $\kappa_{max}\eta_B = 3$ (N= 256^3), and $\kappa_{max}\eta_B = 6$ (N= 512^3). The value of $\langle\chi\rangle$ used in Eq. 3 was obtained from the $\kappa_{max}\eta_B = 6$ simulation, since the highest grid resolution corresponds to best accuracy. The value obtained at this resolution was approximately the same ($\langle\chi'\rangle = 135$) for all the schemes tested.

The effect of numerical diffusion on the spectra is clearly discernible in Figs. 6(a) and 6(b) ($\kappa_{max}\eta_B = 1.5$) for $\kappa\eta \geq 0.4$. The MECH scheme produces a spectrum that is much closer to the expected Kraichnan form, compared to the rest of the schemes. An increase in grid resolution to $\kappa_{max}\eta_B = 3$ (Fig. 6(c), 6(d)) leads to a much better collapse of the spectra of all the schemes tested, and a good agreement with the Kraichnan form in the viscous-diffusive subrange. A further increase from $\kappa_{max}\eta_B = 3$ to $\kappa_{max}\eta_B = 6$, however, leads to only a marginal improvement. Using these observations, it would seem that a grid resolution of at least $\kappa_{max}\eta_B = 3$ is required for the numerical schemes to become independent of discretization errors.

3.2.3 Turbulent Statistics

In addition to recovering the correct spectrum, numerical schemes must also produce accurate turbulent statistics. Models used in reacting turbulent flow often rely heavily on these statistics, espescially at the smallest resolved scales. For instance, the scalar dissipation rate (χ) is one of the main parameters that is widely used in non-premixed combustion models. It is obtained using the equation for scalar variance
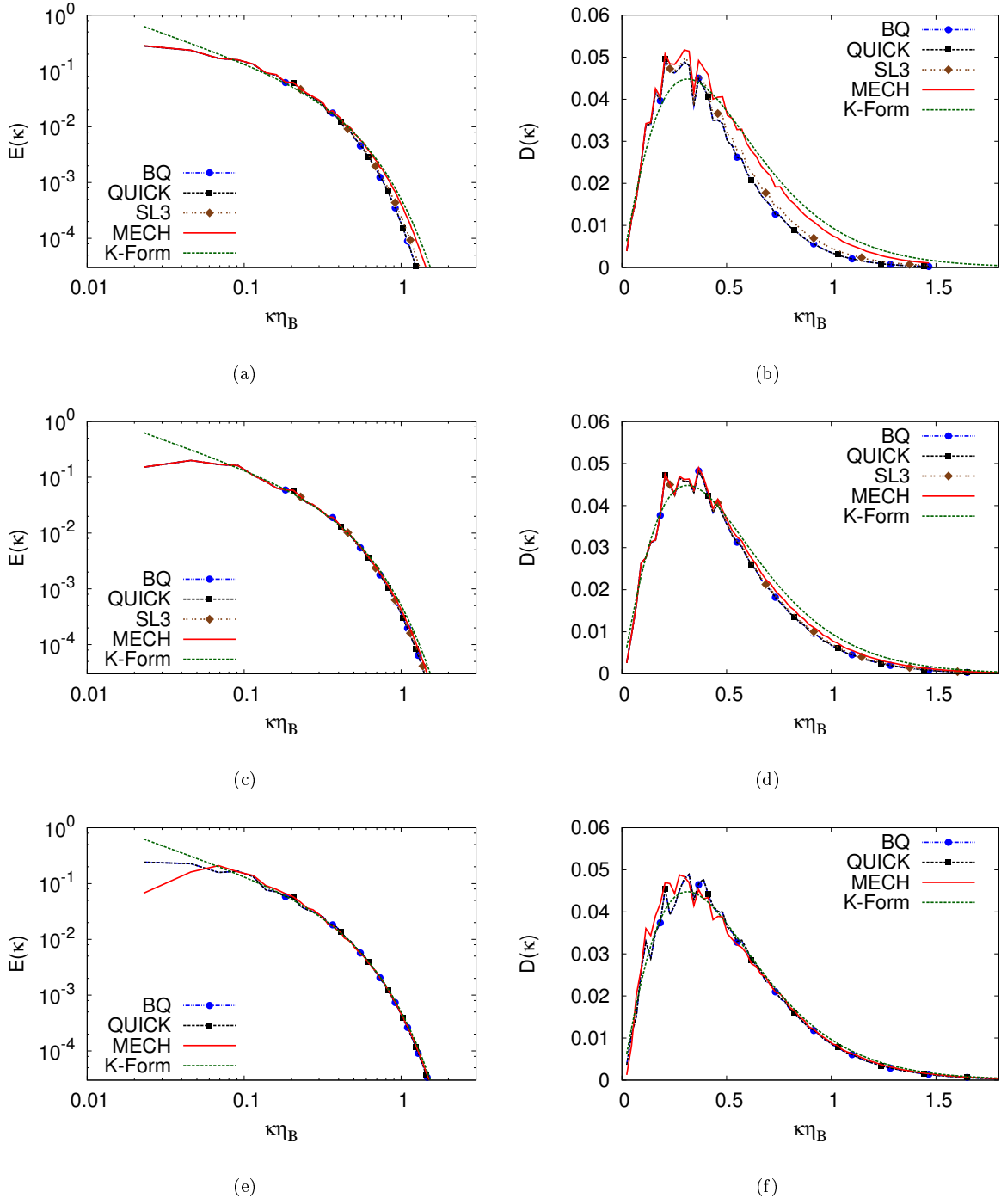
Figure 6: Energy and Dissipation spectra for $Re_\lambda = 30$, Sc=4 ($\eta = 0.0457, \langle \epsilon \rangle = 1.83, \langle \chi' \rangle = 135$) ; [(a), (b) - $\kappa_{max}\eta_B = 1.5$, $N = 128^3$] ; [(c), (d) - $\kappa_{max}\eta_B = 3$, $N = 256^3$] ; [(e), (f) - $\kappa_{max}\eta_B = 6$, $N = 512^3$].
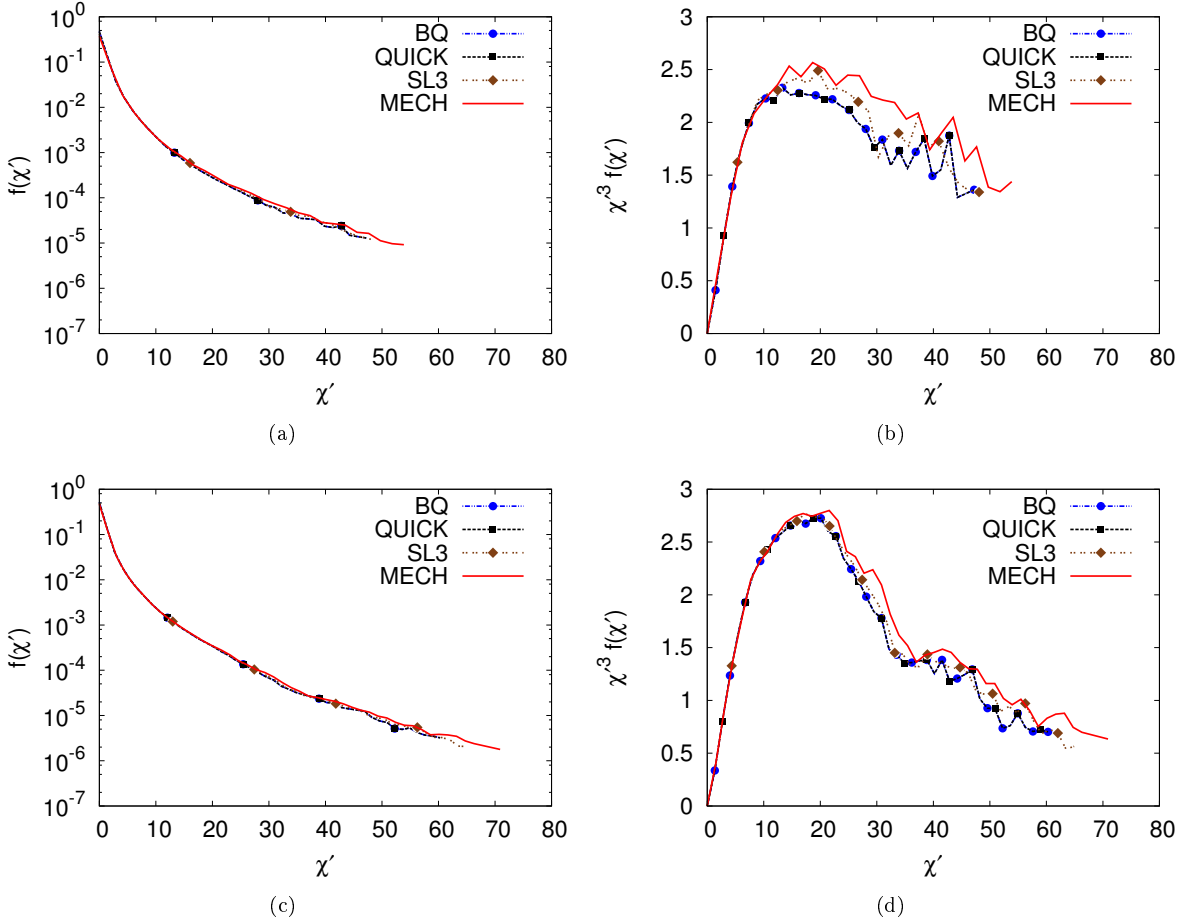
Figure 7: PDF of χ', and plot of $\chi'^3 f(\chi')$ for $Re_\lambda = 30$, $Sc = 4$; [(a), (b) - $\kappa_{max}\eta_B = 1.5$, $N = 128^3$] ; [(c), (d) - $\kappa_{max}\eta_B = 3$, $N = 256^3$].

transport, and is defined as follows:

$$\chi = 2\mathcal{D}|\nabla z|^2 \qquad (4)$$

In the present work, the scalar dissipation rate serves as an indicator of the resolution of the simulations. Since the scalar dissipation rate is directly dependent on the scalar gradients, insufficient resolution will lead to under-prediction, as coarser grids are unable to resolve sharp gradients in the scalar field. Another important turbulent feature that can be discerned using the dissipation rate is intermittency, which is defined as strong, localized, momentary spikes that occur in the scalar and velocity fields. Scalars are known to be more intermittent than the velocity [6], which causes the discretization errors to have an even greater impact on the scalar than on the velocity.

Fig. 7 shows the PDFs of the normalized scalar dissipation rate ($\chi' = \chi/\langle\chi\rangle$, where $\langle\chi\rangle$ is the mean value), and plots of the integrand for its third order moment ($\chi'^3 f(\chi')$). The integrand places a stronger emphasis on the differences between the schemes tested. The 'jaggedness' at larger values of χ' is evidence of statistical variability and intermittency. We note that the integrads are largely identical for $\chi' < 10$, but diverge considerably at higher values (Fig. 7(b)). Grid refinement to $\kappa_{max}\eta_B = 3$ (Fig. 7(d)) leads to better agreement, which is the result of a decrease in discretization error of the numerical schemes. We also see the integrand beginning to convergence to zero at large χ' values, for $\kappa_{max}\eta_B = 3$.

The extent of PDF data available at large values of χ' is indicative of a particular scheme's ability to capture the sharp localized gradients associated with intermittency. We note the expected increase in PDF

Table 1: Data corresponding to PDFs shown in Fig. 7

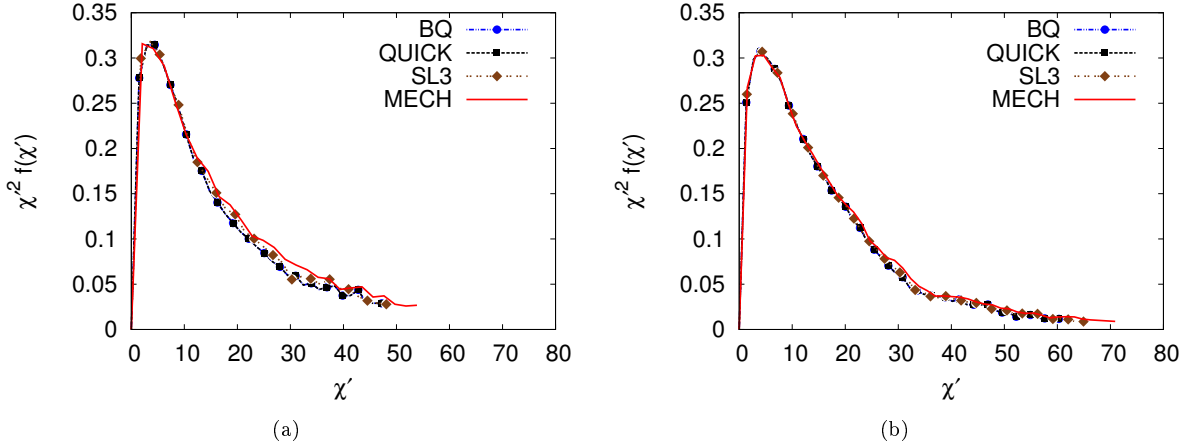| Scheme	$\kappa_{max}\eta_B = 1.5$			$\kappa_{max}\eta_B = 3$		
	$\max(\chi')$	$\langle\chi'^2\rangle$	$\langle\chi'^3\rangle$	$\max(\chi')$	$\langle\chi'^2\rangle$	$\langle\chi'^3\rangle$
QUICK	47.2	5.77	84.7	60.3	6.19	97.3
BQUICK	47.2	5.77	84.7	60.3	6.19	97.3
SL3	48.1	5.97	90.5	64.9	6.32	103.2
MECH	53.9	6.32	105.7	70.9	6.53	112.9

(a)   (b)

Figure 8: Plots of $\chi'^2 f(\chi')$ for (a)$\kappa_{max}\eta_B = 1.5$ and (b)$\kappa_{max}\eta_B = 3$ ($Re_\lambda = 30, Sc = 4$).

data available, upon increasing the grid resolution from $\kappa_{max}\eta = 1.5$ to $\kappa_{max}\eta = 3$ (Fig. 7). Subsequent grid refinements will lead to a further increase in the intermittency registered, however the frequency of occurence of these events (i.e., the associated PDF value) becomes too small to be of practical use. Table 1 lists some relevant statistical data which give us an idea about the performance of each of the schemes. Larger values of the moments correspond to better gradient resolution. We note that MECH is better capable of capturing the intermittency of the scalar field than the other schemes. We also observe a greater variation in the third order moment ($\langle\chi'^3\rangle$), with respect to both the scheme and the resolution used, than in the second order moment ($\langle\chi'^2\rangle$). This is consistent with previous work by Donzis *et. al.* [6], who showed that lower grid resolution has a greater impact on higher order statistics, even when using spectral schemes. They also report an increase in grid resolution sensitivity for successively higher order moments, and that the 'standard' grid resolution of $\kappa_{max}\eta = 1.5$ tends to under-predict higher order statistics such as skewness and kurtosis. However, we suggest that $\kappa_{max}\eta = 1.5$ is sufficient for acceptable accuracy of the first and second order moments (i.e., the mean, and the variance of χ'). We use Fig. 8 to confirm this, where the integrand of the second order moment seems to collapse independently of the numerical scheme used, even for $\kappa_{max}\eta = 1.5$. Increasing grid resolution (Fig. 8(b)) leads to only a marginal improvement in the integrand curve and the variance (Table 1). Thus, a resolution of $\kappa_{max}\eta = 1.5$ might be sufficient for accuracy in most engineering applications, especsially using the MECH scheme.

4   Conclusion

Numerical diffusion introduces appreciable error in simulation of high Schmidt number scalar transport. Using results from simulation of Homogeneous Isotropic Turbulence, we recommend a new grid resolution criterion that accounts for these errors. For standard scalar transport schemes, a resolution of up to $\kappa_{max}\eta_B = 3$ might be necessary to avoid discretization errors. However, it is not always feasible to eliminate these errors by increasing grid resolution, due to the substantial rise in computational cost. A viable alternative to

incurring the high computational cost associated with this grid resolution criterion is to use a scheme with characteristics similar to MECH, at the 'standard' grid resolution of $\kappa_{max}\eta_B = 1.5$. This allows resources to be allocated solely to resolving the physics, and any limitations imposed by the numerical scheme are avoided. We have shown that even though Semi-Lagrangian schemes are non-conservative, the high accuracy and low numerical diffusion associated with them manage to produce small-scale statistics superior to those produced by the non-monotone Eulerian scheme tested. Except for the loss of conservation, SL schemes do not seem to be detrimental to turbulent transport in any way, and are in fact better than comparable Eulerian schemes in retaining overall transport characteristics.

References

[1] P.K. Yeung, S. Xu, D.A. Donzis, and K.R. Sreenivasan. Simulations of three-dimensional turbulent mixing for Schmidt numbers of the order 1000. *Flow Turbul. Combust.*, 72:333, 2004.

[2] Xu-Dong Liu, S. Osher, and T. Chan. Weighted essentially non-oscillatory schemes. *J. Comput. Phys.*, 115(1):200–212, 1994.

[3] M. Herrmann, G. Blanquart, and V. Raman. Flux Corrected Finite Volume Scheme for Preserving Scalar Boundedness in Reacting Large-Eddy Simulations. *AIAA J.*, 44(12):2879–2886, December 2006.

[4] R. J. Leveque. *Finite Volume Methods for Hyperbolic Problems*. Cambridge University Press, Cambridge, 2002.

[5] P. K. Yeung, S. Xu, and K. R. Sreenivasan. Schmidt number effects on turbulent transport with uniform mean scalar gradient. *Phys. Fluids*, 14(12):4178, 2002.

[6] D.A. Donzis and P.K. Yeung. Resolution effects and scaling in numerical simulations of passive scalar mixing in turbulence. *Physica D*, 239:1278, 2010.

[7] G. Brethouwer, J. C. R. Hunt, and F. T. M. Nieuwstadt. Micro-structure and Lagrangian statistics of the scalar field with a mean gradient in isotropic turbulence. *J. Fluid Mech.*, 474:193–225, 2003.

[8] C. Canuto, M.Y. Hussaini, A. Quarteroni, and T. A. Zang. *Spectral Methods: Evolution to Complex Geometries and Applications to Fluid Dynamics*. Scientific Computation. Springer, 2007.

[9] B. Fornberg and J. Zuev. The Runge phenomenon and spatially variable shape parameters in RBF interpolation. *Comput. Math. Appl.*, 54(3):379–398, August 2007.

[10] F. B. Hildebrand. *Introduction to Numerical Analysis*. McGraw-Hill Book Company, New York, NY, second edition, 1974.

[11] R. Bermejo and J. Conde. A Conservative Quasi-Monotone Semi-Lagrangian Scheme. *Mon. Weather Rev.*, 130(2):423–430, 2002.

[12] D. L. Williamson and P. J. Rasch. Two-Dimensional Semi-Lagrangian Transport with Shape-Preserving Interpolation. *Mon. Weather Rev.*, 117, 1989.

[13] B.P. Leonard. A stable and accurate convective modelling procedure based on quadratic upstream interpolation. *Comput. Meth. Appl. M.*, 19:59–98, 1979.

[14] R.J. Purser and L.M. Leslie. An Efficient Interpolation Procedure for High-Order Three-Dimensional Semi-Lagrangian Models. *Mon. Weather Rev.*, 119:2492, 1991.

[15] F.N. Fritsch and R.E. Carlson. Monotone piecewise cubic interpolation. *SIAM J. Numer. Anal.*, 17(2):238–246, 1980.

[16] M. Lentine, J. T. Grétarsson, and R. Fedkiw. An unconditionally stable fully conservative semi-Lagrangian method. *J. Comput. Phys.*, 230(8):2857–2879, 2011.

[17] P. H. Lauritzen. A Stability Analysis of Finite-Volume Advection Schemes Permitting Long Time Steps. *Mon. Weather Rev.*, 135(7):2658–2673, July 2007.

[18] F. Xiao, T. Yabe, X. Peng, and H. Kobayashi. Conservative and oscillation-less atmospheric transport schemes based on rational functions. *J. Geophys. Res.*, 107(D22):1–11, 2002.

[19] K. Alvelius. Random forcing of three-dimensional homogeneous turbulence. *Phys. Fluids*, 11(7):1880, 1999.

[20] R. H. Kraichnan. Small-Scale Structure of a Scalar Field Convected by Turbulence. *Phys. Fluids*, 11(5):945, 1968.

[21] G. K. Batchelor. Small-scale variation of convected quantities like temperature in turbulent fluid: Part 1. General discussion and the case of small conductivity. *J. Fluid Mech.*, 5, 1959.

[22] J. Qian. Viscous range of turbulent scalar of large Prandtl number. *Fluid Dyn. Res.*, 15(2):103–112, February 1995.